

*The 2011 World Congress on Advances in Structural Engineering and Mechanics,  
ASEM11, September 18-22, 2011*

*Organized by the International Association of Structural Engineering and Mechanics (IASSEM) and  
Korea Advanced Institute of Science and Technology (KAIST)*

## **Seismic Soil-Structure Interaction (SSI) Effects for Large-Size Surface and Embedded Nuclear Facility Structures**

**\*Dan M. Ghiocel<sup>1)</sup> and In-Hee Lee<sup>2)</sup>**

<sup>1)</sup> *GP Technologies, Inc., 6 South Main St., 2<sup>nd</sup> Floor, Pittsford, New York 14534, USA,  
email: dan.ghiocel@ghiocel-tech.com*

<sup>2)</sup> *CNG Softek Ltd. Co., #302, CheongSan Bldg., 214-6, Poi-Dong, Gangnam-Gu, Seoul, Korea 135-963,  
email:leeih@cngst.com*

### **ABSTRACT**

The paper discusses a variety of aspects related to SSI modeling and analysis. Specifically, the paper discusses the effects of the 3D seismic wave propagation (incoherent motion) vs. the 1D seismic wave propagation (coherent motion, vertically propagating S and P waves) on SSI response. Theoretical and practical aspects will be presented. The effects of motion incoherency are studied for surface and embedded SSI models, and for rock and soil site conditions. Incoherent motion field was defined based on the 2007 Abrahamson plane-wave coherency models (Abrahamson, 2007). The incoherent SSI analyses were performed using the stochastic simulation approach implemented in the ACS SASSI code (2009). It should be noted that the stochastic simulation approach was validated by EPRI studies (Short, Hardy, Merz and Johnson, 2007) and endorsed by US NRC (2008) for application to seismic analysis of the new nuclear power plant structures within the United States.

Several case studies including simplified SSI models of different nuclear island (NI) designs are presented. For the AP1000 NI complex, the effects of structure-soil-structure interaction (SSSI) are also evaluated for both coherent and incoherent seismic motions. Other case studies include a very large-size auxiliary shear wall building and a deeply embedded UHS type building. The effects of motion incoherency are shown in terms of in-structure response spectra (ISRS), structural forces, and basemat bending moments and forces in embedded walls.

---

<sup>1)</sup> Chief of Engineering with GP Technologies, Inc., New York, and Adjunct Professor with CWRU, Cleveland, US

<sup>2)</sup> President and Engineering Consultant with CNG Softek Ltd. Co., Seoul, Korea

## 1.0 CRITICAL SSI MODELING ASPECTS

Nuclear power plant structures are heavy, massive concrete buildings typically embedded in the surrounding foundation soil. For such heavy and stiff structures the effects of seismic soil-structure soil interaction are significant for all site conditions. It should be noted that seismic SSI effects are significant not only for soil site conditions, but also for rock site conditions. Only, for hard-rock conditions, for sites with very stiff rock with an average shear wave velocity larger than 8,000-9,000 fps, the effects of SSI could be neglected.

The paper focuses on few, selected SSI modeling aspects. The main focus of this paper is on the motion incoherency effects on both surface and embedded nuclear structures for different soil site conditions. Wave passage effects are also included by sensitivity studies. Comparative results are shown for stick and FE structural models, and rigid and flexible basemats. Special case studies are presented on the incoherency effects on seismic pressures for deeply embedded UHS type structure, and structure-soil-structure interaction for a nuclear island (NI) and a neighboring, light Annex Building (AB).

## 2.0 SEISMIC MOTION INCOHERENCY

Seismic motion incoherency is produced by the local random spatial variation of ground motion in horizontal plane in the vicinity of building foundations. To capture the spatial variability of the ground motion in horizontal plane, a stochastic field model is required. Assuming that the spatial variation of the ground motion at different locations could be defined by a homogeneous and isotropic Gaussian stochastic field, its spatial variability is completely defined by its coherence spectrum, or coherence function. Due to the isotropy assumption, the coherence functions defined for any arbitrary direction are the same function called isotropic coherence function. This isotropic coherence function is one-dimensional function with respect to the relative distance between locations, i.e. directional orientation of locations in horizontal plane is not considered.

For a seismic wave stochastic field, with an amplitude denoted  $u(t)$  in time domain and  $U(\omega)$  in frequency domain, the (pair) cross-spectral density (CSD) function for two separated locations on ground surface  $j$  and  $k$ ,  $S_{U_j, U_k}(\omega)$ , is expressed by

$$S_{U_j, U_k}(\omega) = [S_{U_j, U_j}(\omega)S_{U_k, U_k}(\omega)]^{1/2} \Gamma_{U_j, U_k}(\omega) \quad (1)$$

where  $S_{U_j, U_j}(\omega)$  and  $S_{U_k, U_k}(\omega)$  are the power spectral density (PSD) of the seismic motion at locations  $j$  and  $k$ , and  $\Gamma_{U_j, U_k}(\omega)$  is the pair coherence function for locations  $j$  and  $k$ . The coherence function,  $\Gamma_{U_j, U_k}(\omega)$  is a similarity measurement of the two location motions including both the amplitude spatial variation and the wave passage effects.

More generally, the CSD function and coherence function are complex quantities. The complex coherent function is called the “unlagged” coherence function (Abrahamson, 2007). However, in engineering practice, the “lagged” coherence function that is a real and positive quantity defined by the amplitude of the complex coherence function is used instead of the “unlagged” complex coherence function. Further, if the horizontal apparent wave velocity is considered a constant for all frequencies, then, the “plane-wave” coherency model is defined. The plane-wave coherency models, such those provided by Abrahamson (2007), are used in practice in conjunction with the seismic plane-wave propagation SSI codes.

From Eq. 1, it should be noted that the coherence function at any given frequency is identical with the statistical correlation coefficient, sometime also called scaled covariance function, between the two

random variables defined in frequency domain by the amplitudes of ground motion at two locations. This observation suggests that a series of efficient engineering numerical tools developed for digital simulation of stochastic spatial variation fields based on factorization of covariance kernels could be extended for simulation of seismic motion incoherency using factorization of coherence kernels at each frequency.

Currently, based on significant seismological database information recorded in many dense arrays, Abrahamson (2007) defined a set of specific coherency functions for different soil conditions and foundation type for 1) all site conditions and shallow foundations, 2) all site conditions and embedded foundations, 3) for hard-rock sites and shallow and embedded foundations, and 4) soil sites and shallow foundations.

### 3.0 INCOHERENT SSI ANALYSIS METHODOLOGY

In this section, the seismic incoherent SSI analysis methodologies used in the recent EPRI studies (Short, Hardy, Mertz and Johnson, 2006, 2007) that were implemented in the ACS SASSI code (2009) are described hereafter. These methodologies are based on the spectral factorization model proposed by EPRI (Tseng and Lilhanand, 1997). The basic equations shown in this section are described using same notations with Tseng and Lilhanand. The main differences in notation are that for structural degree-of-freedom (dof), we used superscript s instead of subscript s, and for ground motion at interaction nodes we used superscript g instead of subscript g.

#### Incoherent Free-Field Motion

The coherent free-field motion at any interaction node dof k,  $U_k^{g,c}(\omega)$  is computed by:

$$U_k^{g,c}(\omega) = H_k^{g,c}(\omega)U_0^g(\omega) \quad (2)$$

where  $H_k^{g,c}(\omega)$  is the (deterministic) complex coherent ground transfer function vector at interface nodes and  $U_0^g(\omega)$  is the complex Fourier transform of the control motion. Similarly, the incoherent free-field motion at any interaction node dof k,  $U_k^{g,i}(\omega)$  is computed by:

$$U_k^{g,i}(\omega) = \tilde{H}_k^{g,i}(\omega)U_0^g(\omega) \quad (3)$$

where  $\tilde{H}_k^{g,i}(\omega)$  is the (stochastic) incoherent ground transfer function vector at interaction node dofs and  $U_0^g(\omega)$  is the complex Fourier transform of the control motion. The main difference between coherent and incoherent free-field transfer function vectors is that the  $H_k^{g,c}(\omega)$  is deterministic quantity while  $\tilde{H}_k^{g,i}(\omega)$  is a stochastic quantity (the tilda represents a stochastic quantity) that includes deterministic effects due to the seismic plane-wave propagation, but also stochastic effects due to incoherent motion spatial variation in horizontal plane. Thus, the incoherent free-field transfer function at any interaction node can be defined by:

$$\tilde{H}_k^{g,i}(\omega) = S_k(\omega)H_k^{g,c}(\omega) \quad (4)$$

where  $S_k(\omega)$  is a frequency-dependent quantity that includes the effects of the stochastic spatial variation of free-field motion at any interaction node dof k due to incoherency. In fact, in the numerical implementation based on the complex frequency approach,  $S_k(\omega)$  represents the complex Fourier transform of relative spatial random variation of the motion amplitude at the interaction node dof k due to incoherency. Since these relative spatial variations are random,  $S_k(\omega)$  is stochastic in nature. The stochastic  $S_k(\omega)$  can be computed for each interaction node dof k using spectral factorization of coherency matrix computed for all SSI interaction nodes. For any interaction node dof k, the stochastic spatial motion variability transfer function  $\tilde{H}_k^{g,i}(\omega)$  in complex frequency domain is described by the product of the stochastic eigen-series expansion of the spatial incoherent field times the deterministic complex coherent ground motion transfer function:

$$\tilde{H}_k^{g,i}(\omega) = \left[ \sum_{j=1}^M \Phi_{j,k}(\omega) \lambda_j(\omega) \eta_{\theta_j}(\omega) \right] H_k^{g,c}(\omega) \quad (5)$$

where  $\lambda_j(\omega)$  and  $\Phi_{j,k}(\omega)$  are the j-th eigenvalue and the j-th eigenvector component at interaction node k. The factor  $\eta_{\theta_j}(\omega)$  in Eq. 5 is the random phase component associated with the j-th eigenvector that is given by  $\eta_{\theta_j}(\omega) = \exp(i\theta_j)$  in which the random phase angles are assumed to be uniformly distributed over the unit circle. The number of coherency matrix eigenvectors, or incoherent spatial modes, could be either all modes or a reduced number of modes M depending on the eigen-series convergence.

#### Incoherent SSI Response Calculations

For a coherent motion input, assuming a number of interaction nodes equal to N, the complex Fourier SSI response at any structural dof i,  $U_i^{s,c}(\omega)$ , is computed by the superposition of the effects produced by the application of the coherent motion input at each interaction node k:

$$U_i^{s,c}(\omega) = \sum_{k=1}^N H_{i,k}^s(\omega) U_k^{g,c}(\omega) = \sum_{k=1}^N H_{i,k}^s(\omega) H_k^{g,c}(\omega) U_0^g(\omega) \quad (6)$$

where the  $H^s(\omega)$  matrix is the structural complex transfer function matrix given unit inputs at interaction node dofs. The component  $H_{i,k}^s(\omega)$  denotes the complex transfer function for the i-th structural dof if a unit amplitude motion at the k-th interaction node dof is applied. For incoherent motion input, the complex Fourier SSI response at any structural dof i,  $U_i^{s,i}(\omega)$ , is computed similarly by the superposition of the effects produced by the application of the incoherent motion input at each interaction node dof k:

$$U_i^{s,i}(\omega) = \sum_{k=1}^N H_{i,k}^s(\omega) U_k^{g,i}(\omega) = \sum_{k=1}^N H_{i,k}^s(\omega) \left[ \sum_{j=1}^M \Phi_{j,k}(\omega) \lambda_j(\omega) \eta_{\theta_j}(\omega) \right] H_k^{g,c}(\omega) U_0^g(\omega) \quad (7)$$

Two types of incoherent seismic SSI analysis approaches could be used for solving Eq. 7: the stochastic approach and deterministic approach. These approaches were investigated for EPRI (Short, Hardy, Merz and Johnson, 2007). *Stochastic approach* is based simulating random incoherent motion realizations (Simulation Mean in EPRI studies). Using stochastic simulation algorithms, a set of random incoherent motion samples is generated at each foundation SSI interaction nodes. For each incoherent

motion random sample an incoherent SSI analysis is performed. The final mean SSI response is obtained by statistical averaging of SSI response random samples. *Deterministic approach* approximates the mean incoherent SSI response using simple superposition rules of random incoherency mode effects, such as the algebraic sum (AS) (AS in EPRI studies) and the square-root of the sum of square (SRSS) (SRSS in EPRI studies).

It should be noted that for the stochastic simulation approach and the deterministic approach based on linear superposition, the number of extracted coherency matrix eigenvectors, or incoherent spatial modes, can be as large as desired with zero impact on the incoherent SSI analysis run time. By default, all the incoherent spatial modes are included. Consideration of all incoherent spatial modes improves the incoherent SSI accuracy and produces an accurate recovery of the free-field coherency matrix at the interaction nodes; this can be checked for each calculation frequency. The AS approach is fast, much faster than the stochastic approach, and it is easy to use. The SRSS approach is more difficult to apply since has no convergence criteria for the required number of incoherent spatial modes to be considered. It can be applied by a trial-and-error basis. It should also be noted that the SRSS approach requires one SSI analysis for each incoherent mode, that means that is at least several times slower than the AS approach that requires only a single SSI analysis. Also, SRSS neglects the incoherence mode coupling that could be sometime significant, especially for complex structural models.

In the AP1000 NI SSI studies, both stochastic and deterministic incoherent SSI approaches using ACS SASSI code (Ghiocel, Li, Coogler and Tunon-Sanjur, 2009, Ghiocel, Short and Hardy, 2009, 2010, Ghiocel, Li, Brown and Zhang, 2010). In addition to stochastic simulation approach, three deterministic approaches were considered: i) linear superposition, or algebraic sum, of the scaled incoherent spatial modes (AS in EPRI studies), ii) quadratic superposition of the incoherent modal SSI complex response amplitudes (transfer function amplitudes) assuming a zero-phase for the incoherent SSI complex response phase (SRSS in EPRI studies), and iii) quadratic superposition of the incoherent modal SSI complex response amplitudes (transfer function amplitudes) assuming a non-zero phase for the incoherent SSI complex response that is equal to coherent SSI complex response phase (not used in EPRI studies). The last implementation is an alternate version of SRSS approach that does not neglect the complex response phase.

For *rigid foundations* the incoherency-induced stochasticity of the basemat motion is driven by the global or rigid body spatial variations (integral variations) of free-field motion and, therefore, is less complex and random than free-field motion. The rigid foundation motion has a smoothed spatial variation pattern since the kinematic SSI interaction is large. Thus, the differential free-field motions are highly constrained by the rigid basemat, and because of this (rigid body), the foundation motion complexity is highly reduced in comparison with the complexity of the local motion spatial variations. For *flexible foundations*, the incoherency-induced stochasticity of the basemat motion is driven by the local spatial variations of free-field motion. The flexible foundation motion has a less smoothed spatial variation pattern since kinematic SSI is reduced. Thus, the differential free-field motions are less constrained by the basemat, and because of this, the (flexible) foundation motion complexity is similar to the complexity of the local motion spatial variations.

Based on our investigations, we noticed that due to their stochastic modeling simplicity, deterministic SSI approaches are limited to rigid foundation applications, as shown in EPRI studies (Short, Hardy, Mertz and Johnson, 2007). For flexible foundations, the free-field motion local spatial variations are directly transmitted to the flexible basemat motion. For flexible foundations, the stochastic simulation approach is the only choice since it accurately captures the statistical nature of the local free-field motion spatial variations (Ghiocel, Li, Coogler and Tunon-Sanjur, 2009). Deterministic approaches are not capable of capturing accurately the local phasing of the interaction motions for flexible foundation.

Because of this, deterministic approaches could be inaccurate, especially at the corner locations of complex nuclear structures and for flexible foundations, for which the incoherence modal response correlations could be significant in some frequency ranges.

It should be noted that for the final design-basis seismic incoherent SSI analyses, Westinghouse Co. uses the Stochastic Simulation approach for the AP1000 NI complex for both the standard plant design and the site-specific applications (LaPay, 2008, 2011). The same Stochastic Simulation approach is also used by Mitsubishi Heavy Industries for site-specific applications (Mitsuzawa, 2011).

## 2.0 CASE STUDIES

In this section, a number of important SSI modeling aspects related to coherent and incoherent motions are discussed. These includes the effects of i) motion incoherency for different soils, and for surface and embedded NI structures, ii) incoherence modal response coupling, and iii) SSSI between neighboring nuclear buildings.

### AP1000 NI Complex SSI Studies

A number of sensitivity studies were performed for AP1000 NI complex using the simplified multistick SSI model developed by EPRI (Short, Hardy, Mertz and Johnson, 2007). These studies included both isolated surface and embedded SSI models and SSSI models including the coupling through the soil between NI and AB models, as shown in Figure 1 (Ghiocel, Li, Coogler and Tunon-Sanjur, 2009, Ghiocel, Short and Hardy, 2009, 2010, Ghiocel, Li, Brown and Zhang, 2010). The EPRI AP1000 NI stick foundation size was modified from the 150ft x 150ft size to the 158ft x 254ft size that reflects the actual foundation size.

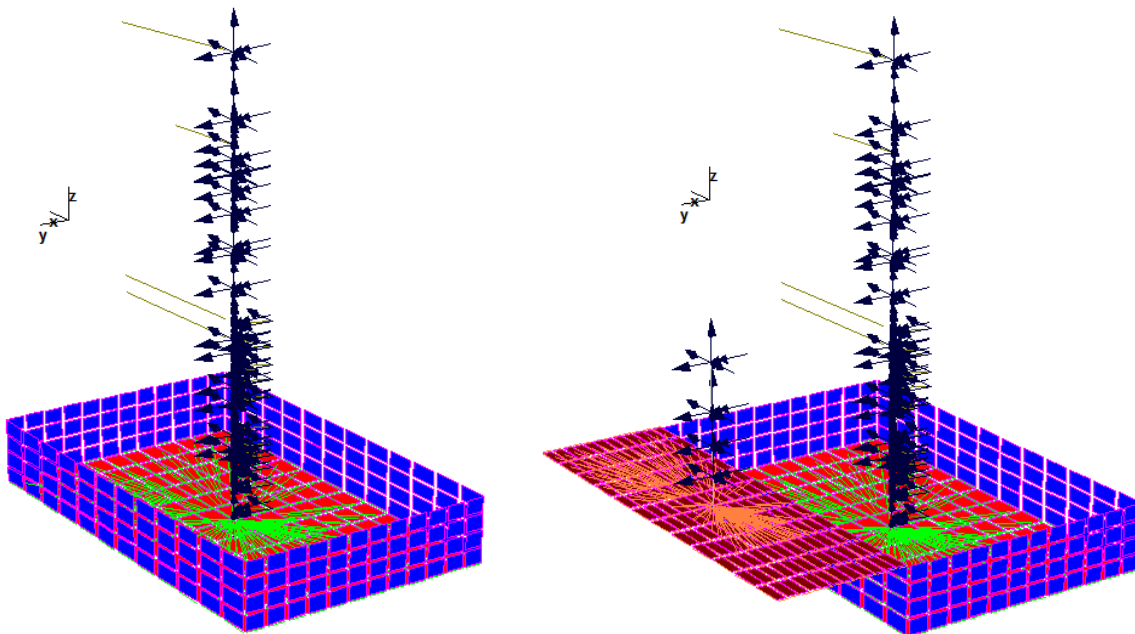


Figure 1 The NI Model (left) and Coupled NI-AB Model (right)

Two different soil conditions were considered. For the original AP1000 NI stick model, the soil layering, seismic input and Abrahamson coherency model were identical with those used as in the EPRI

studies. For the modified AP1000-based stick model with a larger foundation size, the seismic input and soil layering were changed to reflect two extreme soil site conditions: 1) hard-rock site ( $V_s$  about 8,000fps) and 2) soft soil condition ( $V_s$  about 1,000fps). The seismic input was defined by a site-specific ground spectrum that is typical for the hard-rock condition (peak spectral acceleration is in the 20-25 Hz range), and the RG 1.60 spectrum for the soil condition, respectively. The 2007 Abrahamson coherency model for hard-rock and soil sites (Abrahamson, 2007) were applied. The control motion was defined at ground surface. The two versions of the AP1000-based stick models were considered with no embedment, as in EPRI studies, and with 35 ft and 50 ft embedment depths, respectively.

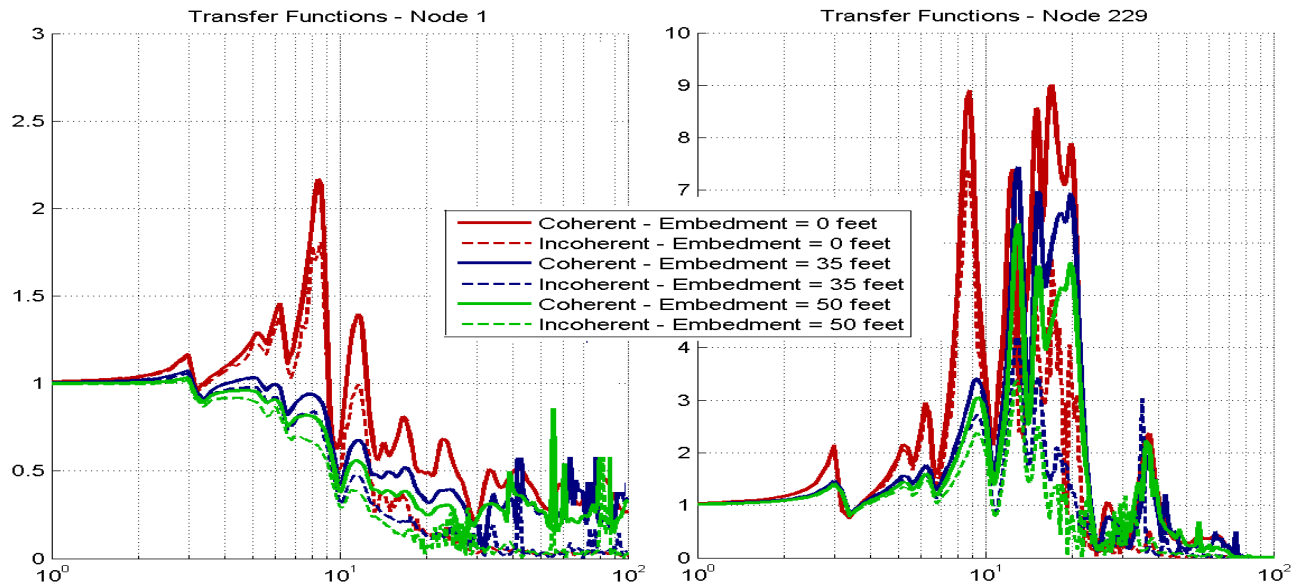


Figure 2 Embedment and Motion Incoherency Effects on Acceleration Transfer Function (ATF) Amplitudes at Basemat Center (Node 1) and at the Top of CIS (Node 229)

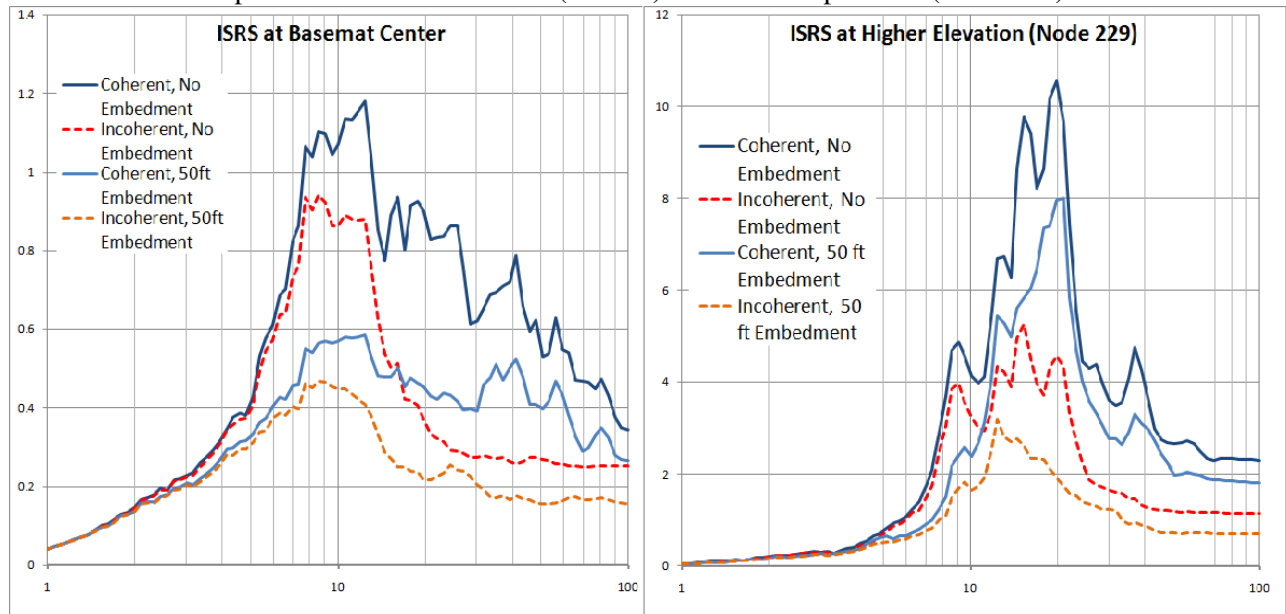


Figure 3 Embedment and Motion Incoherency Effects on 5% Damping ISRS at Basemat Center (Node 1) and at the Top of CIS (Node 229)

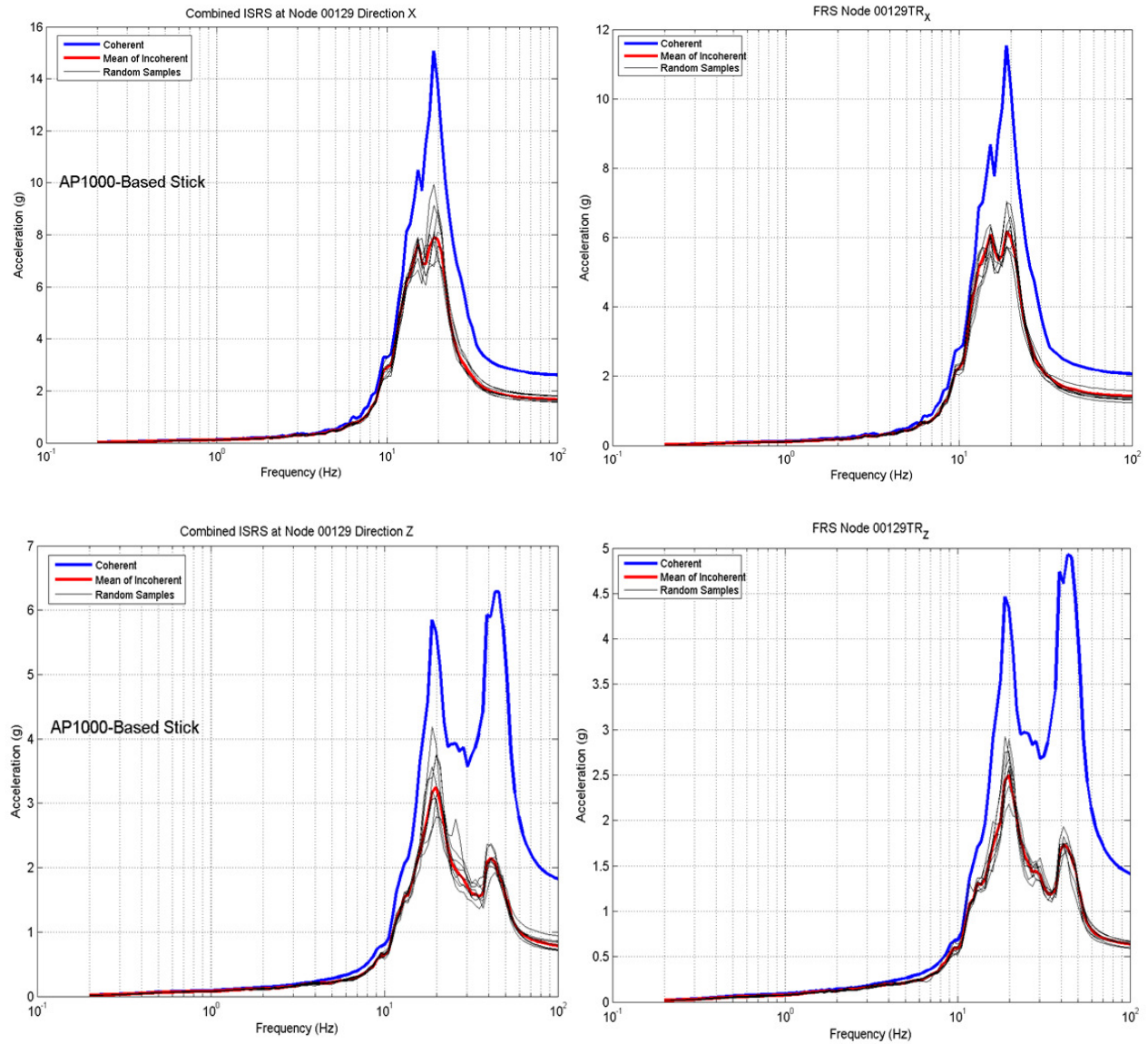


Figure 4 Motion Incoherency Effects for Non-Embedded (left plots) and 40ft Embedded (right plots) AP1000 NI Stick on 5% Damping ISRS at Top of CIS for the Hard-Rock Conditions (Vs of 8,000fps) with the Hard-Rock Seismic Input for X (top) and Z (bottom) Directions.

Figures 2 and 3 show the computed (mean) incoherent and coherent acceleration transfer function amplitudes and 5% damping ISRS in the X direction at the basemat center (node 1) and at the outrigger extending 75ft in X direction from the top of the containment internal structure (CIS) of the unmodified EPRI AP1000-based stick model (node 229). The same seismic input and soft rock layering used in the EPRI studies was considered. Comparisons are for no embedment, 35ft and 50ft embedments. The 2005 Abrahamson coherency model developed for all sites was employed for both non-embedded and embedded SSI models. It should be noted that the favorable embedment effects to reduce the SSI responses are dominant up to 12-15 Hz frequency, above which the motion incoherency effects become more dominant. As shown in Figure 3, in the high-frequency range the ISRS reductions due to motion incoherency could be more than 50%.

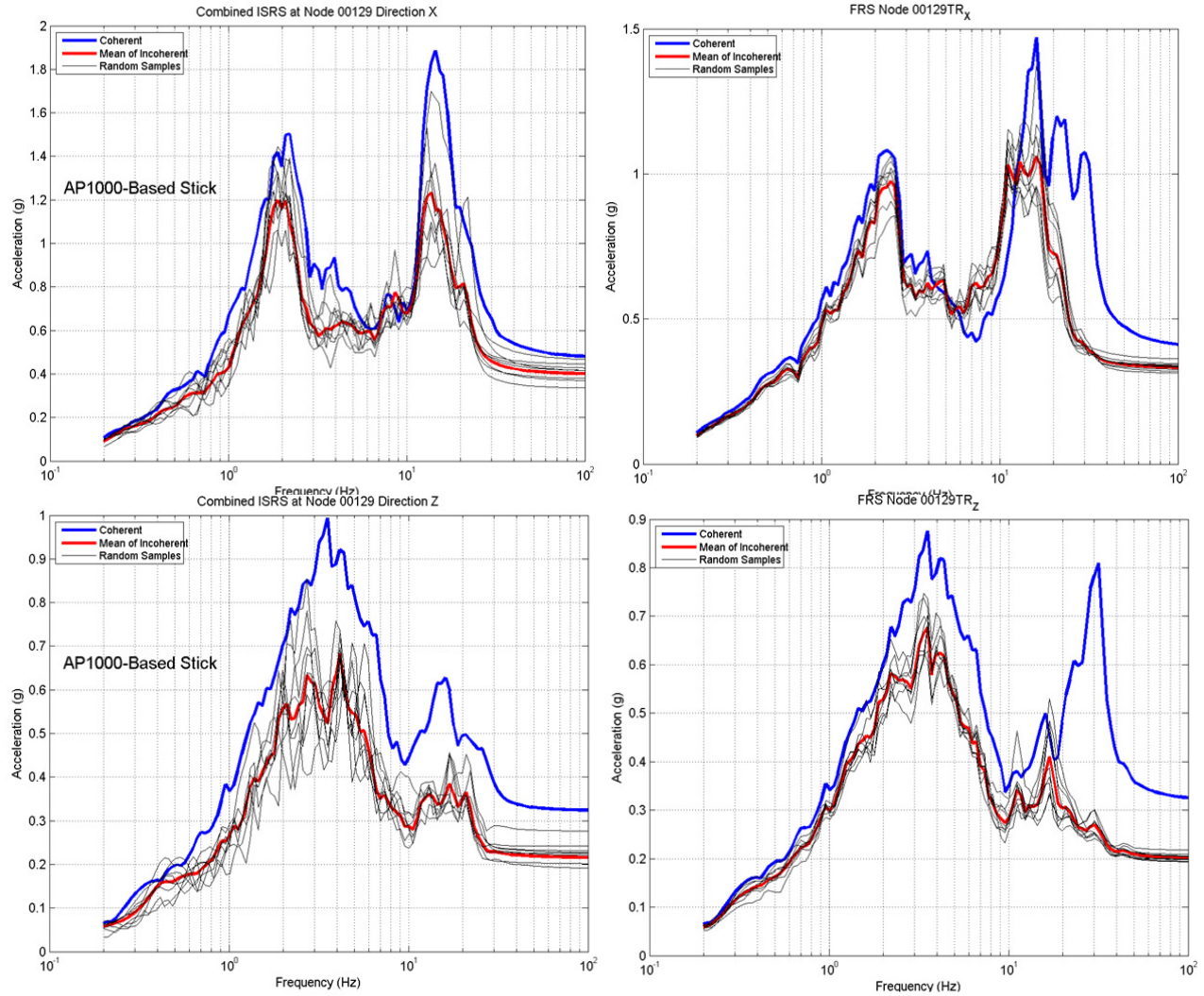


Figure 5 Motion Incoherency Effects for Non-Embedded (left plots) and 40ft Embedded (right plots) AP1000 NI Stick on 5% Damping ISRS at Top of CIS for the Soft Soil Conditions ( $V_s$  of 1,000fps) with the RG 1.60 Seismic Input for X (top) and Z (bottom) Directions

Figures 4 and 5 show the effect on motion incoherency on the 5% damping ISRS computed for the modified AP1000 NI stick model at the outrigger extending 10 ft in Y direction from the top of CIS (node 129) for both hard-rock and soft-soil site conditions. The SSI analysis inputs for the two site conditions, including the coherence functions. By studying Figures 4 and 5, there are several visible aspects are remarked:

- The effects embedment and motion incoherency on SSI responses are significant for both the hard-rock and soft-soil sites. It should be noted that even for the hard-rock site with  $V_s$  of 8,000fps (about 2,500m/s), the embedment effect still produces a 20% ISRS reduction. More generally, the motion incoherency effects are significantly larger for hard-rock sites than soil-sites. However, as shown in Figure 5 for ISRS in Z-direction, the reduction due incoherence could be also large for soil sites if higher frequency responses are present.

- The effects of embedment and motion incoherency on SSI response have simple trends for the hard-rock condition and complex trends for the soft-soil condition. For soft soil condition, the embedment effect indicates a slightly different dynamic behavior of the SSI model that is visible under both coherent and incoherent inputs. For example, in the X and Z directions, the coherent ISRS show that the embedment amplifies the SSI mode responses at 25 Hz and 30 Hz frequencies.
- The motion incoherency effects are larger for higher frequency ranges. The magnitudes of the ISRS reductions depend significantly on soil site conditions. For the hard-rock site, the motion incoherency effects reduce the SSI response for all frequency ranges, but more drastically in the high-frequency range above 10-12 Hz. For the soft-soil condition, the motion incoherency effects manifest significantly starting at lower frequency ranges, well below 10 Hz when the soft soil coherence function is used.

As mentioned earlier, the AP1000 studies have also investigated the effects of the seismic structure-soil-structure interaction (SSSI) for the EPRI AP1000 NI complex and Annex Building (AB) (Ghiocel, Li, Brown and Zhang, 2010). The AB structure is assumed to be a light and stiff structure with a mass of only fraction of the mass of the AP1000 NI structures (basemat mats not included). To investigate the SSSI effects three computational SSI models were employed: 1) Isolated NI stick model, 2) Isolated AB stick model and 3) Coupled NI-AB stick model. Each of these SSI models was run separately and their results were compared.

For the SSSI analysis, the two soil site conditions was considered to be a two layer soil deposit, namely, a uniform top soil layer on a hard-rock foundation. The uniform top soil layer is a 40 ft backfill soil layer that has a shear wave velocity  $V_s = 1,000$  fps. The hard-rock foundation below 40ft depth has a shear wave velocity  $V_s = 8,000$  fps. The AP1000 NI complex is fully embedded in the backfill layer and sits on the hard-rock foundation (at Elevation 60 ft). The AB structure has no embedment and sits on the backfill layer at the ground surface level nearby the NI complex (at Elevation 100 ft). Figure 1 shows the isolated NI model and the coupled NI-AB model. The seismic input is defined by a site specific high-frequency UHRS input that is the same as that used in the EPRI studies (Short, Hardy, Mertz and Johnson, 2007) anchored to a ZPA of 0.30g. The site-specific UHS input was defined at the top of the rock foundation.

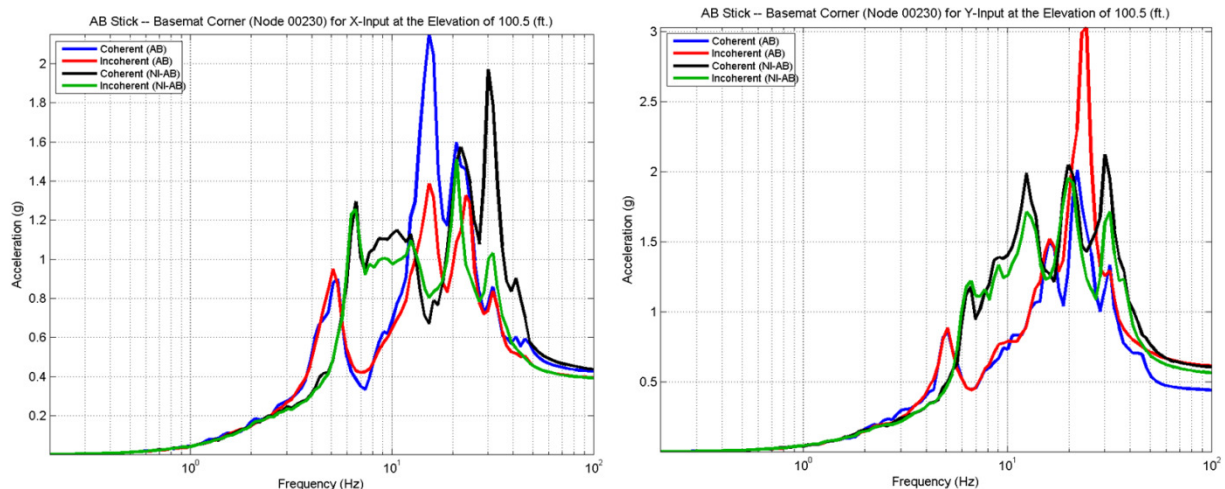


Figure 6 Comparative 5% Damping ISRS for Isolated AB Model and NI-AB Coupled Model in X (left) and Y (right) Directions at Basemat Corner, Elevation 100 ft

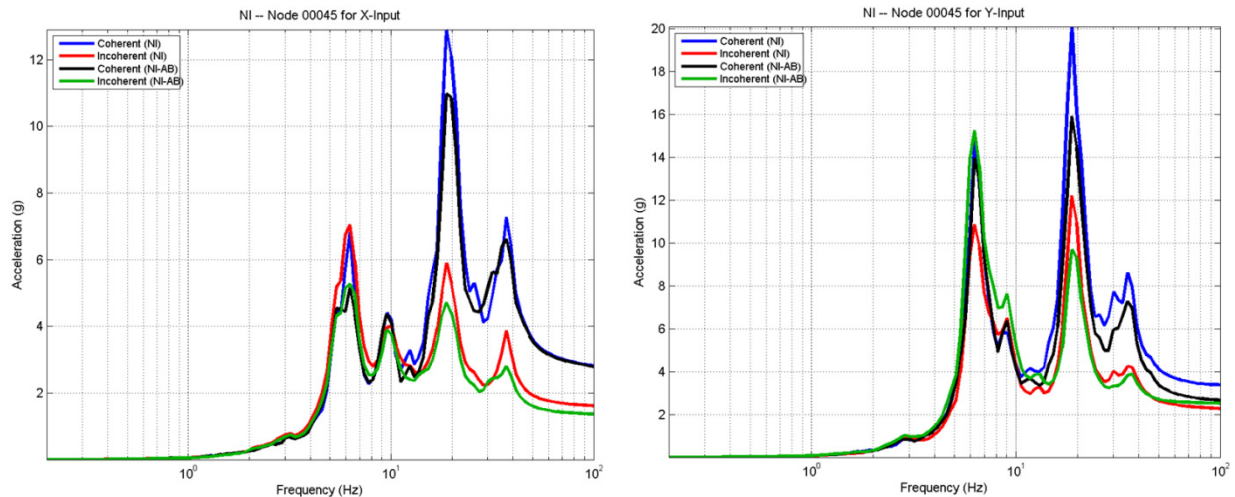


Figure 7 Comparative 5% Damping ISRS for NI Model and Coupled NI-AB Model in X (left) and Y (right) Directions at Top of SCV Stick at Elevation 282 ft

The results include both coherent and incoherent analysis results for the three SSI models. Figures 6 and 7 shows the ISRS computed for isolated and coupled models for the AB and NI structures. Figure 6 shows the main ISRS spectral peak at 5.0 Hz that corresponds to the global SSI mode of the isolated AB structure on the soil foundation is “vanished” due to the dynamic coupling with the NI complex. Instead, there are new ISRS peaks at higher frequencies. These spectral peaks are produced by the dynamic coupling with the NI complex that excites higher frequency modes of the AB structure. At the higher elevations in the AB structure, the ISRS computed using the coupled NI-AB model could be larger due to the higher-order modes that are excited due to the nearby presence of the NI complex. It should be noted that the global SSI vibration mode of AB structure on the foundation soil that is dominant at 5.0 Hz for the isolated AB model is apparently not excited or only very minimally in the coupled NI-AB model.

Figure 7 shows the computed ISRS for the isolated NI model and the coupled NI-AB model at the top of the SCV (steel containment vessel) stick at Elevation 282 ft and the ASB stick at Elevation 333 ft. The ISRS computed in the X and Y directions are shown. It should be noted that the isolated NI model provides typically slightly larger ISRS than the coupled NI-AB model.

For the investigated case study, the effects of SSSI are relatively minor for the NI complex structures, but significant for the AB structure. Specifically, for both coherent and incoherent inputs, the SSSI effects reduce largely the shear forces in the AB structure and almost negligibly in the NI complex structures.

### Large-Size Shearwall Structure with Flexible Basemat

The large-size shearwall structure study uses a generic modular configuration building with a horizontal foundation size of 460ft x 320ft as shown in Figure 8 (Ghiocel, Short and Hardy, 2010).

The large-size shearwall structure is assumed to be founded on a rock site with  $V_s$  of 4,500 fps. The seismic input was defined by the HRHF input used also to the AP1000 stick model. The 2007 Abrahamson hard-rock coherency model was used. The seismic input was assumed to consists of vertically propagating S waves for horizontal motion components and P waves for vertical motion component.

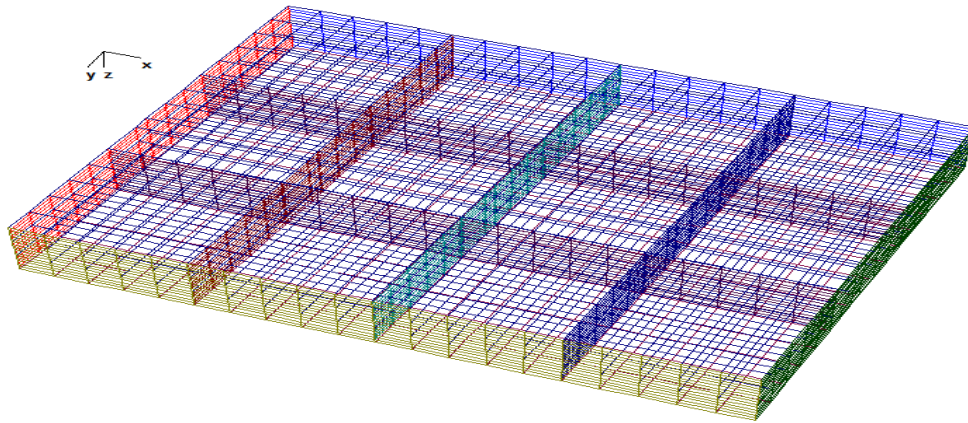
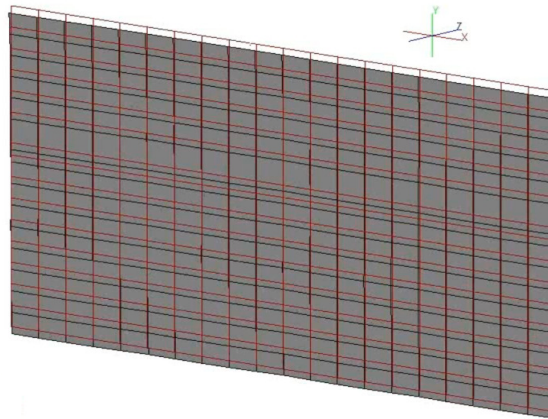
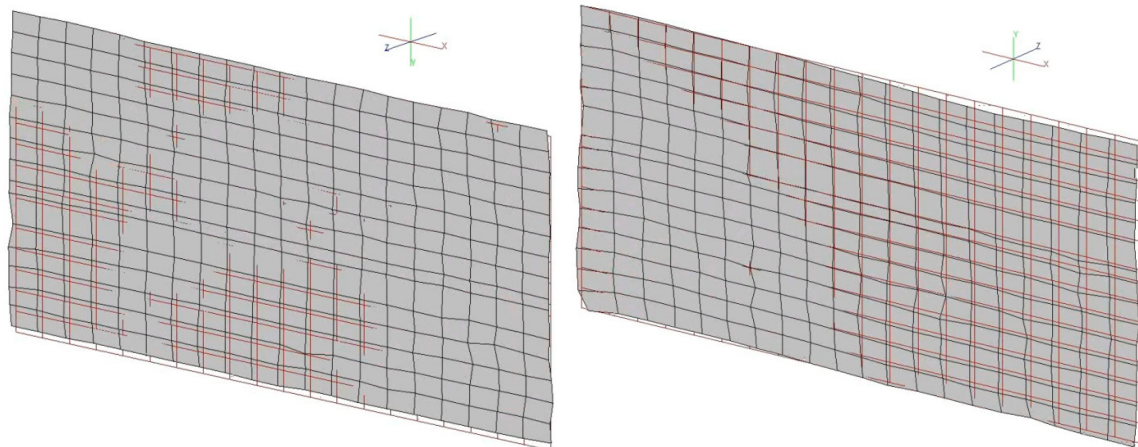


Figure 8 Large-Size Shear Wall Structure With An Area of 460ft x 320ft

For this large-size structure we also considered the wave passage effects. Since we assumed that the soil deposit has a soil layering inclination in a direction that makes about 30 degree with longitudinal axis of the foundation, we considered a horizontal apparent wave speed of 6,000 fps in a 30 degree oblique direction. The 6,000 fps is extreme low apparent speed that was considered to produce an upperbound of the wave passage effects.



a) Baselab Coherent SSI Accelerations



b) Baselab Incoherent SSI Accelerations Without (left) and With Wave Passage (right)

Figure 9 Basemat SSI Acceleration “Deformed Shape” Frozen At Arbitrary Time

Figure 9 shows the instantaneous SSI acceleration distributions in the basemat at arbitrary time by the deformed shape of the baselab. The baselab was isolated from the rest of the structure. The baselab deformed plots were computed for the coherent input (a), incoherent input (b, left) and incoherent plus wave passage input (b, right). It should be noted that for the large-size and flexible basemat, the effects of incoherency appear to be important. Based on the Figure 9 plots, intuitively, it is expected that the baselab maximum bending moments increase due to incoherency and wave passage. It is clear from Figure 9 that traditional coherent analysis that assumes that the entire 450 ft x 350 ft soil area under the foundation moves as a “rigid body” is unrealistic and against recorded evidence in seismographic dense arrays. This “rigid body” assumption for soil motion could underevaluate significantly the bending of the baselab. We noticed that incoherency and wave passage effects could increase the baselab bending moments by 50% or more.

The above remarks are confirmed in Figures 10 and 11. Figures 10 and 11 compare the incoherent and coherent maximum bending moments in the large-size shear wall flexible basemats. It should be noted that the incoherent bending moments are up to 3-5 larger than the coherent bending moments. This significant increase of basemat bending moments due to the motion incoherency is produced by the larger induced SSI displacements due to kinematic SSI effects.

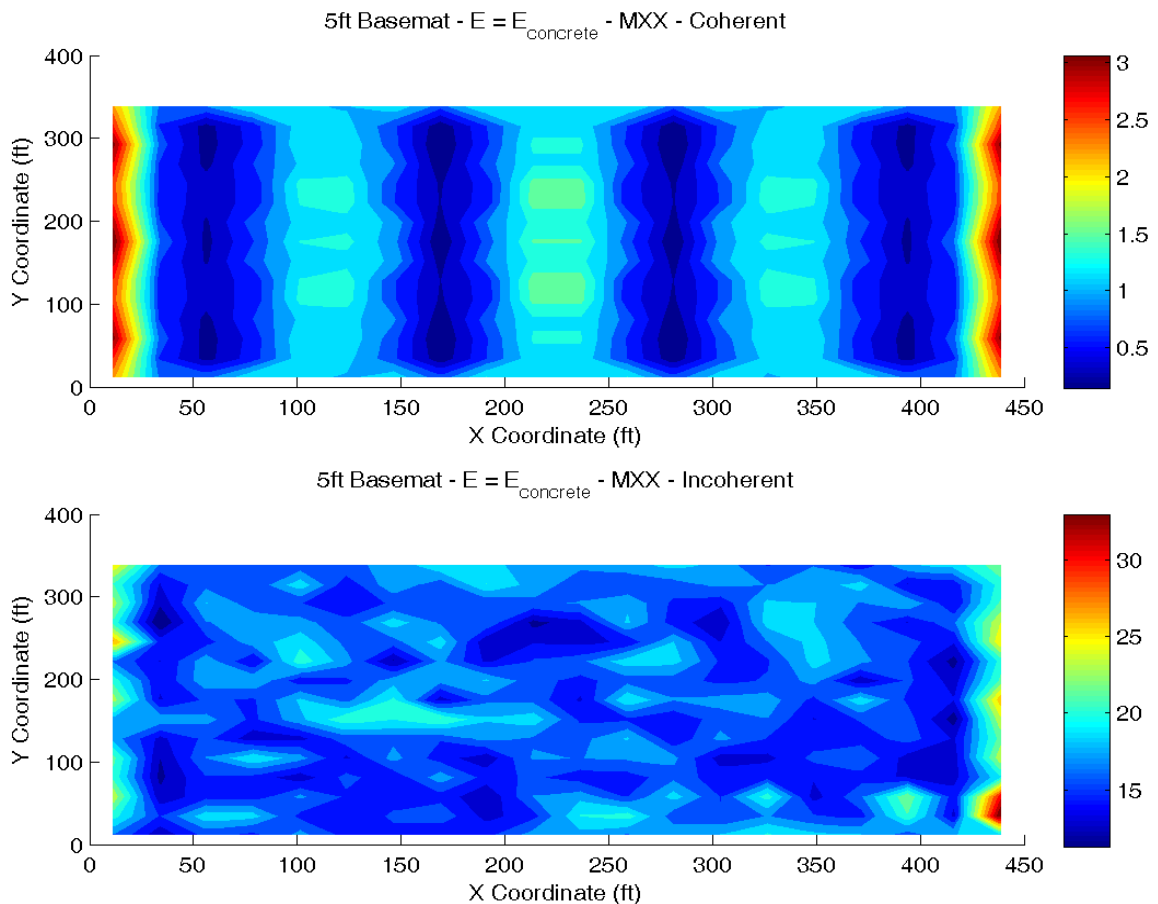


Figure 10 Coherent vs. Incoherent Maximum Bending Moments MXX

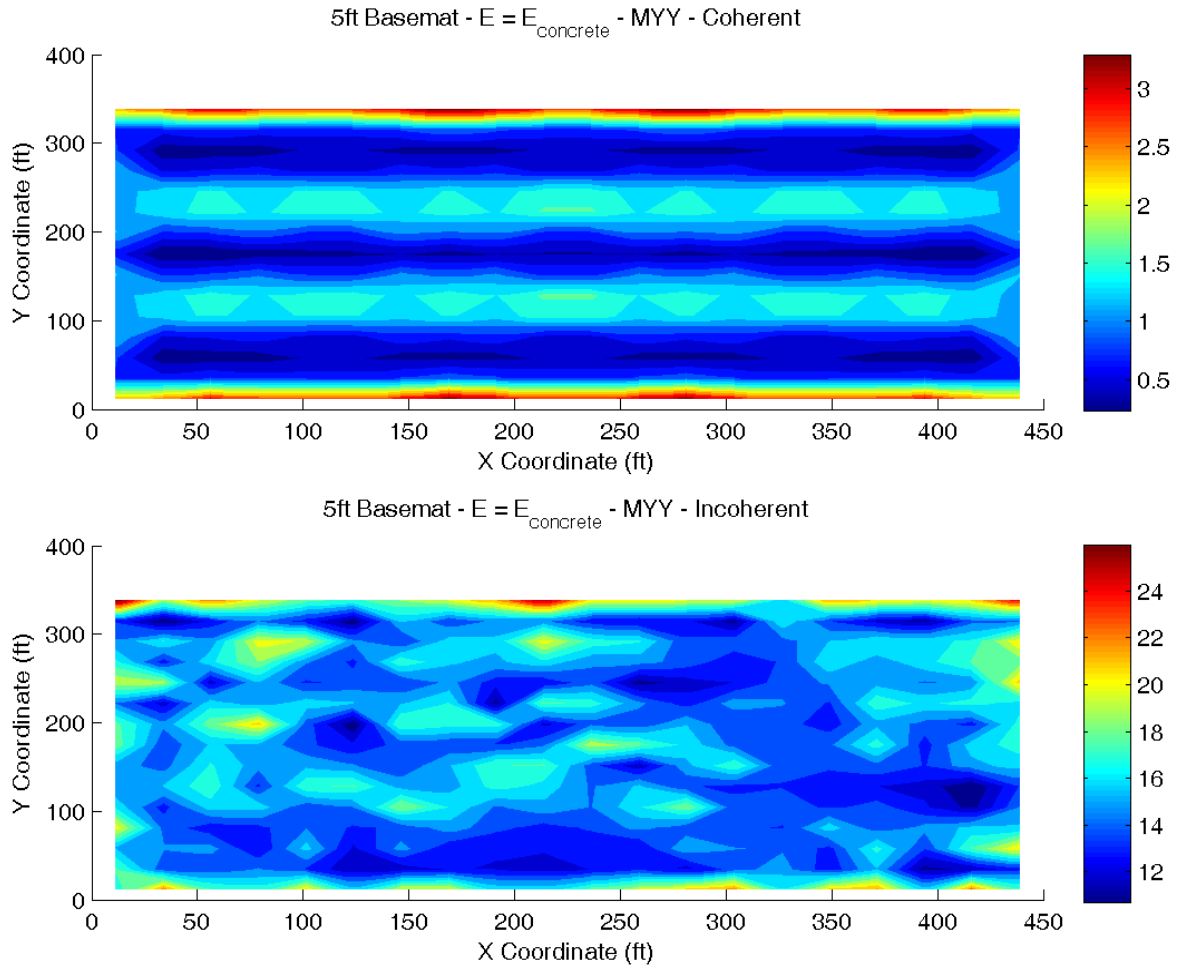


Figure 11 Coherent vs. Incoherent Maximum Bending Moments  $M_{YY}$

It should be that the computed seismic basemat bending moments from SSI analysis include the contributions of both the primary stresses due to structural loads, and the secondary stresses due to SSI induced displacements. The current engineering design procedures for conventional building concrete footers below columns or wall lines or basemats do not consider the secondary stresses produced by the SSI induced displacements. The neglect of the secondary stresses could produce a large under evaluation of the elastic bending moments in the basemat. However, it should be noted that for the ultimate strength design approach used in the ASCE code for concrete design, the effects of the secondary stresses could be neglected if the basemat has sufficient ductility to accommodate the SSI induced displacements.

Table 1 shows the effects of incoherency and wave passage on the forces and moments in the external transverse shearwall. Table 1 shows that incoherency could increase the out-of plane bending moments in shearwall by 10% if no wave passage is considered, and by 30% if passage is included. The axial and shear forces could increase by 10-15% if incoherency and wave passage are included. More research is needed to quantify for practice these qualitative aspects.

Element	Analysis	Va	Value	Axial	Shear	Moment
	coh		max	35.398	28.541	3.476
			max	26.987	24.671	3.809
external wall	incoh	Infinity	ratio	0.762	0.864	1.096
		6000	ratio	1.139	1.099	1.287
	coh		max	19.313	45.618	2.874
			max	14.940	35.326	2.242
interior wall	incoh	Infinity	ratio	0.774	0.774	0.780
		6000	ratio	0.715	0.716	0.630

Tabel 1 Comparison of Coherent and Incoherent Shell Element In-Plane Forces and Out-of-Plane Bending Moments

### Deeply Embedded Flexible Concrete Pool Structure

The concrete pool structure model used in this study is shown in Figure 12 (Ghiocel, Short and Hardy, 2010). The foundation size in horizontal plane is 80ft x 50 ft. The embedment is 30 ft. The pool structure is a very flexible structure since is an open box structure.

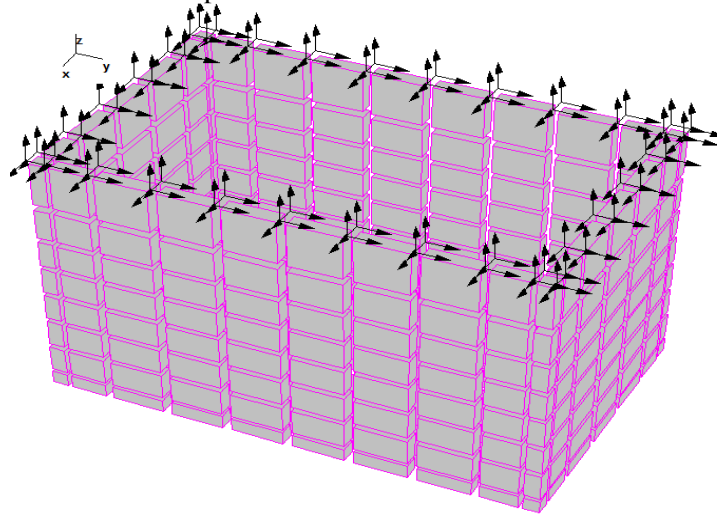


Figure 12 30 ft Embedded Flexible Concrete Pool Structure with A Size of 80ft x 50ft

Figure 13 shows the coherent and incoherent structural acceleration deformed shapes at an arbitrary time. It should be noted the structural deformation patterns show that for incoherent inputs in addition to regular mode of vibration patterns there are present random patterns due to presence of short wave length random components. Thus, the differential soil motions due to incoherency create local differential soil pressures that affect the vibration shape of the concrete structure.

Figure 14 shows the membrane stresses in the 30 ft embedded concrete pool structure. It is obvious that the incoherent stresses are much lower on the top of the pool structure due to reduced inertial forces at the top due to incoherency. However, at lower levels under the ground surface, the incoherent, random short wavelength components could produce locally larger stresses in the concrete structure due to differential

soil motions. It is believed that the wave scattering phenomenon is largely affected by incoherency due to the presence of out-of-phase motion components. More research is needed to quantify for engineering practice these important aspects.

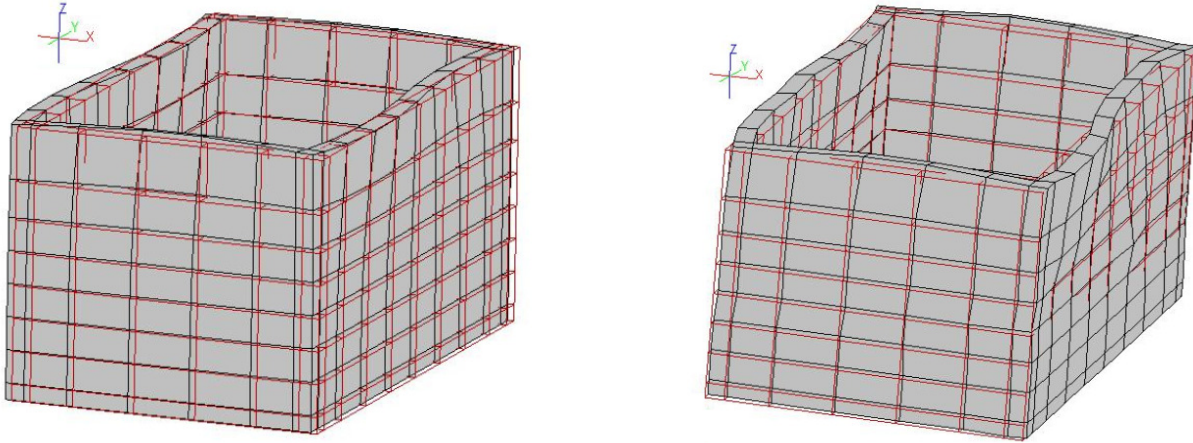


Figure 13 SSI Accelerations at Arbitrary Time for Coherent (left) and Incoherent (right) Inputs

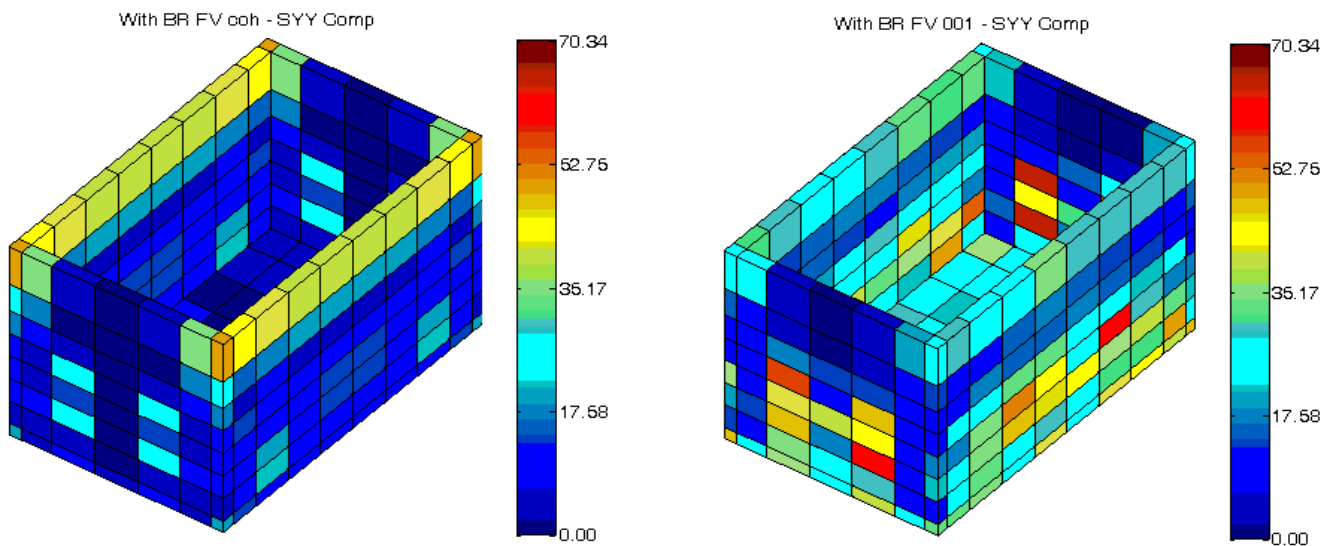


Figure 14 Coherent (left) and Incoherent (right) Membrane Forces in the 30 ft Embedded Concrete Structure Walls (embedment covers the lower 5 element layers)

#### 4.0 CONCLUSIONS

Key the conclusions on the effect of motion incoherency are: 1) Reduces the ISRS amplitudes in high-frequency range. For rock sites, large ISRS amplitude reductions of 2-3 times are possible; 2) Increases bending moments in basemats; 3) For large foundation sizes, could also increase the shear wall forces in external walls; 4) The inclusion of wave passage effects could be favorable for interior shear walls and detrimental for external walls located at the longitudinal edges; 5) For deeply embedded structures, the incoherency effects are to reduce the global resultant of the local soil pressures, but locally might produce “hot spot” pressures due to short wavelength soil motion components. Wave scattering effects around deeply embedded structures are sensitive to motion incoherency.

## 5.0 REFERENCES

- Abrahamson, N. (2007). "Effects of Seismic Motion Incoherency Effects" Electric Power Research Institute, Palo Alto, CA and US Department of Energy, Germantown, MD, Report No. TR-1015110, December 20
- ACS SASSI Version 2.3.0 (2009) "An Advanced Computational Software for 3D Dynamic Analysis Including Soil Structure Interaction", User Manuals, Ghiocel Predictive Technologies, Inc., Rochester, New York, USA, June 15 (<http://www.ghiocel-tech.com/engineeringTools.html>)
- Ghiocel, D.M, Li, D., Brown, N. and Zhang, J.J. (2010) "EPRI AP1000 NI Model Studies on Seismic Structure-Soil-Structure Interaction (SSSI) Effects", Proceedings of the OECD NEA SSI Workshop, Ottawa, October 6-8
- Ghiocel, D.M., Li.,D., Tunon-Sanjur, L. (2009). "Seismic Motion Incoherency Effects for AP1000 Nuclear Island Complex", The 20th Structure Mechanics in Reactor Technology, Proceedings of SMiRT20 Conference, Paper 1852, Helsinki, August 10-14
- Ghiocel, D.M., Short, S. and Hardy, G. (2010). "Seismic Motion Incoherency Effects for Nuclear Complex Structures On Different Soil Site Conditions", Proceedings of the OECD NEA/IAEA SSI Workshop, Ottawa, October 6-8
- Ghiocel, D.M., Short, S. and Hardy, G. (2009). "Seismic Motion Incoherency Effects on SSI Response of Nuclear Islands with Significant Mass Eccentricities and Different Embedment Levels", The 20th Structure Mechanics in Reactor Technology, Proceedings of SMiRT20 Conference, Paper 1853, Helsinki, August 10-14
- LaPay, W.S. (2008). Westinghouse AP1000 Design Control Documentation, Chapter 3 on Design of Structures, Components, Equipment and Systems, Appendix 3I on Evaluation for High-Frequency Inputs, US NRC Abrams Database Document # ML103480529
- LaPay, W.S. (2011). Westinghouse AP100 Technical COLA Report APP-GW-GLR-1 15 Rev. 3 on "Effect of High Frequency Seismic Content on SSCs", US NRC Abrams Database Document # ML110691052
- Mitsusawa, D. (2010). Mitsubishi Heavy Industries, US-APWR Seismic Design Bases and Technical COLA Reports, available from US NRC Abrams Database
- Short, S.A., G.S. Hardy, K.L. Merz, and J.J. Johnson (2007). "Validation of CLASSI and SASSI to Treat Seismic Wave Incoherence in SSI Analysis of Nuclear Power Plant Structures", Electric Power Research Institute, Palo Alto, CA and US Department of Energy, Germantown, MD, Report No. TR-1015111, November 30
- Tseng and Lilhanand (1997). "Soil-Structure Interaction Analysis Incorporating Spatial Incoherence of Ground Motions", Electric Power Research Institute, Palo Alto, CA and US Department of Energy, Germantown, MD, Report No. TR-102631, November
- USNRC (2008). Final Interim Staff Guidance DC/COL-ISG-01 "Seismic Issues Associated with High Frequency Ground Motion in in Design Certification and Combined License Applications", USNRC, Rockville, MD, May 2008 (<http://www.nrc.gov/reading-rm/doc-collections/isg/col-app-design-cert.html>)